Int. J. Heat Mass Transfer. Vol. 36, No. 8, pp. 2039–2049, 1993
Printed in Great Britain

0017-9310/93 $6.00 + 0.00


# Critical heat flux measurements in a round tube for CFCs and CFC alternatives

R. M. TAIN and S. C. CHENG
Department of Mechanical Engineering, University of Ottawa, Ottawa, Ontario, Canada K1N 6N5

and

D. C. GROENEVELD
Chalk River Laboratories, Atomic Energy of Canada Limited, Chalk River, Ontario, Canada K0J 1J0

(*Received* 17 *July* 1992 *and in final form* 27 *October* 1992)

**Abstract**—Critical heat flux (CHF) measurements have been conducted for HFC-134a, HCFC-123, HCFC-22, CFC-12 and CFC-11 in a multi-fluid loop. The test pressures are up to 2 MPa (corresponding to water equivalent pressure of 7–10 MPa) and mass fluxes from 1000 to 4000 kg $m^{-2}$ $s^{-1}$. The heated length is adjustable from 0.5 to 1 m, the I.D. of the tubular test section is 4.2 mm, and the critical quality varies from 0.07 to 0.6. The parametric trends of test results are examined and the test results show good agreement with existing CHF prediction methods. It also provides confirmation that CFC alternatives such as HFC-134a, HCFC-123 and HCFC-22 can be used with confidence as reliable CHF modelling fluids.

## INTRODUCTION

THE CRITICAL heat flux is the heat flux at which a sudden deterioration of heat transfer rate occurs. For a heat-flux-controlled surface, the surface temperature will rise rapidly and may cause a physical failure, or 'burnout'. CHF investigations may be divided into two fundamental areas: (i) pool boiling CHF, where the heated surface is submerged in a static liquid pool, and (ii) flow boiling CHF, where the heated surface is a channel wall confining the flow or is surrounded by a flow stream. The present work is aimed at the latter one, particularly for flow in uniformly-heated round tubes.

It has been widely recognized that the CHF mechanism which occurs at subcooled or low quality flow conditions (characterized by a transition from nucleate boiling to film boiling) differs from that in high quality flow condition (characterized by an annular film dryout). The physical models for CHF prediction are usually based on the particular CHF mechanism. Whalley *et al.* [1, 2] presented a model for annular flow. Weisman and Pei [3] developed a model for low quality CHF and Lee and Mudawwar's [4] and Katto's [5–7] models are for subcooled flow. The models usually predict CHF regardless of the type of fluid. However, most models require empirical constants which are optimized from experimental CHF data.

There are many empirical prediction methods which have been developed by correlating the available CHF data. Some of them are in dimensionless form so that they can be used for different types of fluid. The accuracies of empirical methods are tolerable, but most of them only apply to a narrow parameter range and for particular flow geometries. Groeneveld *et al.*'s [8] standard table for CHF prediction of water in round tubes covers a very wide range of quality, mass flux and pressure and is considered accurate and reliable (based on 15 000 CHF data). By using the correction factors, this standard table can predict CHF in various flow geometries, e.g. rod bundle, etc., in different flow orientations, and in flow channels with a non-uniform heat flux distribution. Employing the scaling laws from the fluid-to-fluid modelling technique, (e.g. Ahmad [9] and Katto and Ohno [10]) Groeneveld *et al.* [11] converted their standard CHF table for water into a dimensionless form and obtained satisfactory prediction when compared with Weisman and Pei's [3] and Katto and Ohno's [10] prediction methods against the CHF data for various fluids. Shah [12] presented a graphical correlation to predict CHF covering 11 fluids for conditions from subcooled to high quality flows. Later, Shah [13] improved his previous work by extending the fluid types to 23 and by permitting computerized calculation from the graphical correlation. His improved general correlation also covers a very wide range and yields satisfactory prediction against some selected data bases.

CHF experiments have been conducted in many laboratories using various fluids. Most of the CHF data were obtained for water because of the importance of CHF in the design and safety analysis of nuclear reactors. Since full-scale CHF experiments using a nuclear reactor core are impossible, smaller

## NOMENCLATURE

| | |
|---|---|
| $Bo$ | boiling number |
| $Cp_f$ | specific heat of saturated liquid |
| $D$ and I.D. | inside diameter |
| $Fr$ | Froude number |
| $G$ | mass flux |
| $G^*$ | non-dimensional mass flux |
| $h_{exit}$ | total enthalpy at the exit of test section |
| $h_f$ | liquid saturated enthalpy |
| $h_{in}$ | total enthalpy at the inlet of test section |
| $K_f$ | thermal conductivity of saturated liquid |
| $L$ and H.L. | heated length |
| $\dot{m}$ | mass flow rate |
| O.D. | outside diameter |
| $P$ | pressure |
| $Pe$ | Peclet number |
| $P_r$ | reduced pressure |
| $\dot{q}$ | test section power |
| $Q$ | volumetric flow rate |
| $X$ | thermodynamic quality |
| $X_c$ | critical quality |
| $Y$ | Shah's correlating parameter |
| $z$ | length in axial direction. |

Greek symbols

| | |
|---|---|
| $\gamma$ | $\lvert\partial(\rho_f/\rho_g)/\partial P\rvert_{saturation}$ |
| $\Delta H_i$ | inlet subcooling enthalpy |
| $\lambda$ | enthalpy of evaporation |
| $\mu_f$ | saturated liquid viscosity |
| $\mu_g$ | saturated vapour viscosity |
| $\rho_f$ | saturated liquid density |
| $\rho_g$ | saturated vapour density |
| $\sigma$ | surface tension |
| $\phi_c$ | critical heat flux |
| $\psi_{CHF}$ | Ahmad's scaling parameter (general expression) |
| $\psi_k$ | Katto's scaling parameter |
| $\psi_\gamma$ | Ahmad's scaling parameter based on $\gamma$ |
| $\psi_\sigma$ | Ahmad's scaling parameter based on $\sigma$. |

scale CHF tests on electrically-heated fuel-bundle simulators are usually performed in experimental rigs. Because of the high latent heat and high critical pressure of water, such CHF experiments are still very expensive, especially for complex geometries. Therefore, the CHF fluid modelling technique has been used from the consideration of cost, time and less severe test conditions, e.g. lower pressure, temperature and heat flux. From the literature, refrigerants (chloroflourocarbons or CFCs) have been used as working fluids in most CHF modelling tests because of their lower latent heat and lower critical pressure compared with water. An example for typical equivalent conditions for water and CFC-12, HCFC-22, HCFC-123 and HFC-134a is given in Table 1.

Because of the less severe test conditions and the much lower test section power requirements, the cost for CHF testing with CFCs is only a fraction of the cost of equivalent tests using water. However, CFC-11, CFC-12 and some other members of CFC family have been found harmful to the environment by depleting the ozone layer. Therefore, an assessment of CFC alternatives, including an assessment of the CHF behaviour, has begun. New fluids such as HCFC-123 and HFC-134a have been developed having a zero or very low ozone depletion potential; the thermophysical properties of HCFC-123 and HFC-134a are close to CFC-11 and CFC-12, respectively. Table 2 summarizes the basic properties of HCFC-123, CFC-11, HFC-134a, CFC-12 and HCFC-22, and Table 3 is the summary of the environmental characteristics of some CFCs and several promising alternatives.

For refrigeration, air-conditioning and heat pump applications, it is likely that HFC-134a and HCFC-123 will replace CFC-12 and CFC-11, respectively. Furthermore, HCFC-22 is considered to be a temporary replacement fluid for CFC-12 during a transition period. The present work is to conduct systematic CHF measurements with HFC-134a, HCFC-123 and HCFC-22 and to examine the suitability of CFC alternatives as new modelling fluids. For the purpose of comparison, CHF measurements for CFC-12 and CFC-11 have also been performed.

## LOOP DESCRIPTION

The CHF test for CFCs and CFC alternatives were performed in the Multi-fluid Boiling Heat Transfer Loop at University of Ottawa. The loop schematic is illustrated in Fig. 1. Because of the low latent heat of these fluids, the power required for the loop is less than 5 kW, and the mass flux can reach 4000 kg $m^{-2}$ $s^{-1}$ or more, depending on the pump capacity. The volume of this loop when filled is less than 3 l. Such small volume results in a fast responding loop as well

Table 1. Equivalent CHF test conditions for water, CFC-12, HCFC-123, HCFC-22 and HFC-134a

| Parameter | Water | CFC-12 | HCFC-22 | HCFC-123 | HFC-134a |
|---|---|---|---|---|---|
| Pressure (MPa) | 6.89 | 1.07 | 1.34 | 0.98 | 1.13 |
| Temperature (°C) | 265 | 43 | 34.5 | 110 | 44 |
| Mass flux (kg $m^{-2}$ $s^{-1}$) | 2640 | 2047 | 2000 | 1915 | 1828 |
| Test section power (kW) | 26.5 | 1.78 | 2.41 | 1.57 | 1.95 |

Table 2. Physical properties of HCFC-123, CFC-11, HFC-134a, CFC-12 and HCFC-22 (Du Pont data)

| Properties | HCFC-123 | CFC-11 | HFC-134a | CFC-12 | HCFC-22 |
|---|---|---|---|---|---|
| Chemical formula | $CHCl_2CF_3$ | $CCl_3F$ | $CH_2FCF_3$ | $CCl_2F_2$ | $CHClF_2$ |
| Molecular weight | 152.9 | 137.4 | 102.0 | 120.9 | 96.47 |
| Boiling point at 1 atm (°C) | 27.6 | 23.8 | −25.5 | −29.8 | −40.8 |
| Freezing point (°C) | −107 | −111 | −101 | −158 | −160 |
| Critical temperature (°C) | 185 | 198.1 | 100.6 | 112.0 | 96.15 |
| Critical pressure (MPa) | 3.61 | 4.41 | 3.95 | 4.12 | 4.97 |
| Critical density (kg $m^{-3}$) | 583.4 | 554.2 | 488.5 | 557.4 | 513.0 |
| Liquid density at 25°C (kg $m^{-3}$) | 1461 | 1476 | 1203 | 1311 | 1190 |
| Vapour pressure at 25°C (kPa) | 91.7 | 105.6 | 661.9 | 651.6 | 1040 |
| Evaporation heat at boiling point of 1 atm (J $g^{-1}$) | 169.9 | 180.4 | 219.8 | 165.3 | 182.5 |

Table 3. Environmental characteristics of regulated CFCs and several promising alternatives (Watanabe [14])

| Refrigerant | Atmospheric liftetime (yr)† | ODP‡ | GWP§ |
|---|---|---|---|
| CFC-11 | 65 | 1.0 | 1.0 |
| CFC-12 | 120 | 0.9–1.0 | 2.8–3.4 |
| CFC-113 | 90 | 0.8–0.9 | 1.3–1.4 |
| CFC-114 | 180 | 0.6–0.8 | 3.7–4.1 |
| CFC-115 | 380 | 0.3–0.5 | 7.4–7.6 |
| HCFC-123 | 1–4 | 0.013–0.022 | 0.017–0.02 |
| HCFC-124 | — | 0.016–0.024 | 0.092–0.1 |
| HFC-125 | — | 0 | 0.51–0.65 |
| HFC-134a | 6 | 0 | 0.24–0.29 |
| HCFC-22 | 20 | 0.04–0.06 | 0.32–0.37 |

† Time required for a chemical compound to reduce the concentration to 1/e (37%) of its original value.

‡ Ozone depletion potential (relative to CFC-11, which is assigned the value 1).

§ Globe warming potential (relative to CFC-11, which is assigned the value 1).

as savings in cost. The size of the main body of the loop is 80 cm deep, 100 cm wide and 170 cm high (without including the height of pressurizer). The pressure desired for testing these fluids is about 2 MPa or less, simulating water for up to 10 MPa. However, a generous safety margin is applied and the loop is designed to sustain pressures up to 3.45 MPa. Most parts of the loop are made of stainless steel except the heat exchanger and some minor connections, which are made of brass, and the test section, which is made of Inconel.

The main components of this loop are pumps, flow meter, preheater, test section, heat exchanger and pressurizer. Note that the two gear pumps are connected in series in order to obtain twice the pump head for the same flow rate. The loop pressure is adjusted by the pressurizer which contains a heater and a cooling coil. By adding heater power, the liquid will boil so that the pressure in the loop will increase; and by reducing the heater power or increasing the water flow rate in the cooling coil, the pressure in the loop will decrease. The preheater is used to adjust the flow temperature at the inlet of test section. A detailed sketch of the test section is shown in Fig. 2. The test

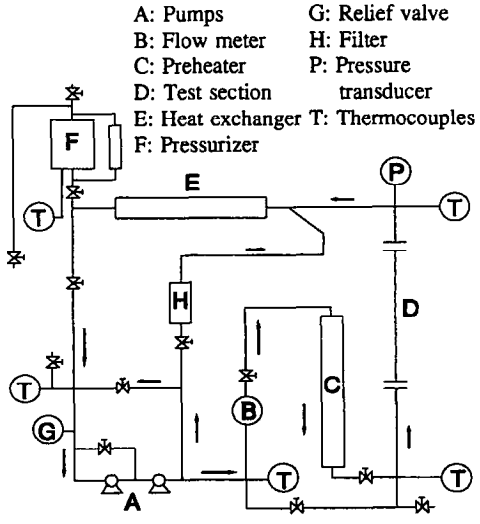


FIG. 1. Outline sketch of the test loop.

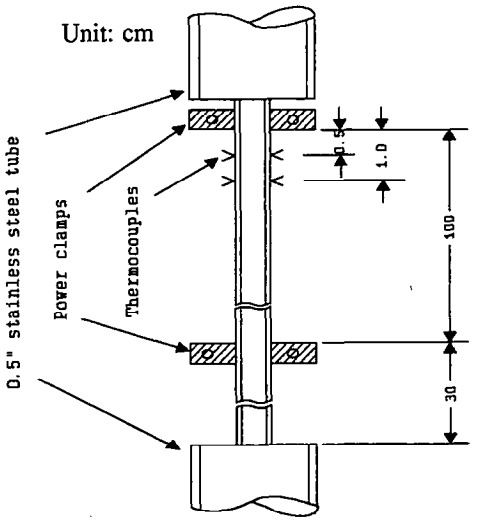


FIG. 2. Sketch of the test section.

section is made of an alloy of Inconel 718 with 4.2 mm I.D. and 4.6. mm O.D.; its heated length can be changed simply by moving the lower power clamp. The wall temperatures near the exit of the test section are measured by K-type, sheathed thermocouples which are ungrounded and fixed to the test section by wooden clips.

## OPERATING PROCEDURE

While the flow is circulating in the loop, the powers of the preheater, the test section and the heater inside the pressurizer are turned on to adjust the system temperature and pressure. The test section power is raised rapidly to about 80% of the CHF power, beyond which the power is slowly increased until CHF occurs. When CHF is observed, the wall temperature at the exit of the test section increases rapidly as seen from a recorder trace. The test section power is subsequently reduced to 80–95% of the CHF power and the flow conditions are adjusted for the next CHF test. Table 4 shows the parameter matrix of CHF tests for CFCs and CFC alternatives.

## MEASUREMENT UNCERTAINTIES

The estimates of measurement uncertainty were based on the manufacturers' specifications and the calibration procedures. The errors of the thermocouple measurement at the inlet and outlet of the test section were calibrated to be 0.2°C by an electrical equivalent of an ice bath. The pressure transducer was calibrated to be 0.6% of R.M.S. error for a full range by the manufacturer. Since the flow at the test-section outlet is in the saturation condition, the fluid properties are calculated based on the temperature measurement. The saturation pressure measurement, thus, is used as a check for the saturation temperature measurement. The flow meter was calibrated to be 1.06% of R.M.S. error by using water. From the manufacturer, no correction factor will be used if the flow meter is used for the fluid other than water as long as the specific weight of the fluid is not far from that of water. The stability of the D.C. power supply is 0.04 V for voltage mode and 0.63 A for current mode. The heat balance test for the test section also has been found to be 1.9% of R.M.S. deviation with respect to the power, flow rate and temperature measurements.

## TEST RESULTS

*Data reduction*

CHF is primarily a function of $P$ (pressure), $G$ (mass flux), $D$ (diameter) and $X_e$ (critical quality). $P$ is measured directly while $G$ and $X_e$ are calculated from other parameters (temperature, pressure, etc.):

$$G = \frac{\dot{m}}{A} = \frac{4}{\pi}\frac{\rho Q}{D^2} \tag{1}$$

$$X_e = \frac{h_{exit} - h_f}{\lambda} \tag{2}$$

where

$$h_{exit} = h_{in} + \frac{\dot{q}}{\dot{m}} \tag{3}$$

and $h_f$ and $\lambda$ are based on outlet pressure. CHF is obtained from

$$\text{CHF} = \phi_c = \frac{\dot{q}}{\pi DL}. \tag{4}$$

The symbols are defined in the nomenclature. The thermophysical properties required for present work are based on Hammouda [15], Hammouda *et al.* [16] and McLinden *et al.* [17].

*Observed parametric trends*

Table 5 is a summary of the test results from the present work. Note that the CHF data of HCFC-123 for the high pressure condition (water-equivalent pressure of 10 MPa) was not obtained because the high saturation temperature (130°C) creates a cooling problem in the heat exchanger. For a similar reason, very few CHF data for CFC-11 were taken. The CHF data are plotted against the critical quality ($X_e$) as shown in Figs. 3 and 4 for various pressures, heated lengths and dimensionless mass fluxes, $\psi_k$ (to be defined in equation (15)). These figures show that all fluids display similar trends of increasing CHF with decreasing $X_e$. At low pressure conditions as shown in Fig. 3, little difference in CHF values with respect to $X_e$ between HFC-134a and CFC-12 has been

Table 4. Parameter matrix of CHF test for CFCs and CFC alternatives

| Parameter | Parameter matrix |
|---|---|
| Pressure for water at $\rho_f/\rho_g$ = 20.3 and 12.4 (MPa) | 7 and 10 |
| Pressure for HFC-134a at $\rho_f/\rho_g$ = 20.3 and 12.4 (MPa) | 1.13 and 1.66 |
| Pressure for HCFC-22 at $\rho_f/\rho_g$ = 20.3 and 12.4 (MPa) | 1.34 and 1.96 |
| Pressure for CFC-12 at $\rho_f/\rho_g$ = 20.3 and 12.4 (MPa) | 1.06 and 1.58 |
| Pressure for HCFC-123 at $\rho_f/\rho_g$ = 20.3 (MPa) | 0.98 |
| Pressure for CFC-11 at $\rho_f/\rho_g$ = 20.3 and 12.4 (MPa) | 1.13 and 1.65 |
| Mass flux (kg m$^{-2}$ s$^{-1}$) | 1000–4000 |
| Inlet subcooling temperatures (°C) | 2–40 |
| Heated length (cm) | 50–100 |
| Inside diameter (mm) | 4.2 |

Table 5. CHF test results for CFCs and CFC alternatives

| Fluid | $P$ (MPa) | $G$ (Mg m$^{-2}$ s$^{-1}$) | $L/D$ | No. of data | $X_c$ | CHF (kW m$^{-2}$) |
|---|---|---|---|---|---|---|
| HFC-134a | 1.13(7)† | 1.38–3.69 | 185–238 | 65 | 0.11–0.48 | 110–250 |
| HFC-134a | 1.66(10) | 1.37–3.66 | 185–238 | 73 | 0.09–0.40 | 85–254 |
| HCFC-22 | 1.34(7) | 1.50–4.00 | 119–238 | 68 | 0.15–0.50 | 140–270 |
| HCFC-22 | 1.96(10) | 1.50–4.00 | 185–238 | 61 | 0.12–0.40 | 100–250 |
| CFC-12 | 1.06(7) | 1.53–4.08 | 185–238 | 58 | 0.13–0.49 | 104–215 |
| CFC-12 | 1.58(10) | 1.53–4.09 | 185–238 | 69 | 0.12–0.40 | 74–200 |
| HCFC-123 | 0.98(7) | 1.45–3.86 | 185–238 | 60 | 0.07–0.46 | 100–252 |
| CFC-11 | 1.13(7) | 1.05 | 238 | 1 | 0.58 | 103 |
| CFC-11 | 1.65(10) | 1.05–2.17 | 238 | 6 | 0.17–0.47 | 80–150 |

† The number inside the parentheses referred to water-equivalent pressure.

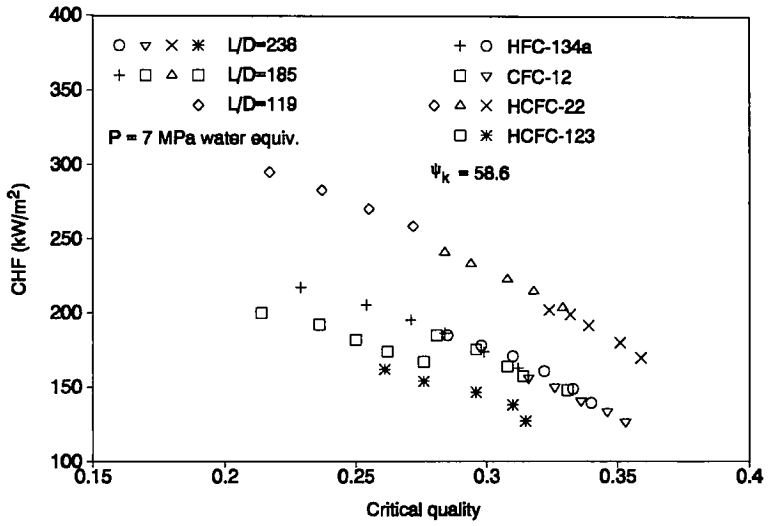


(a)

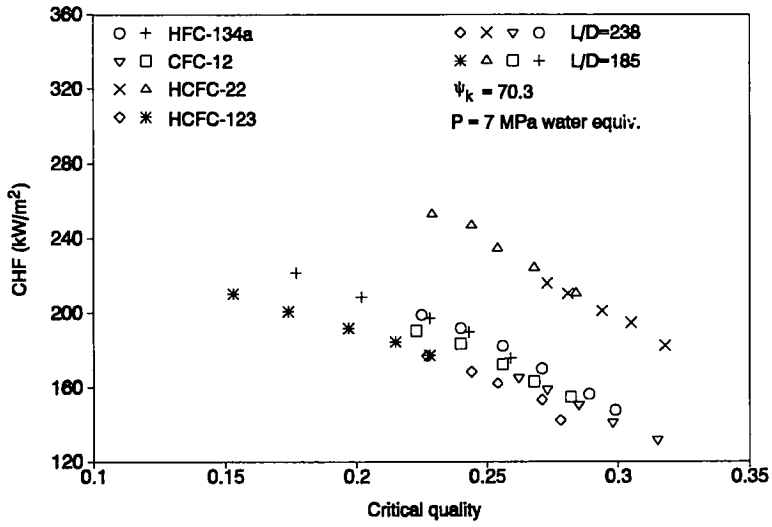


(b)

FIG. 3. Effect of quality on CHF for CFC and CFC alternatives at 7 MPa water-equivalent pressure: (a) $\psi_k = 58.6$, (b) $\psi_k = 70.3$.

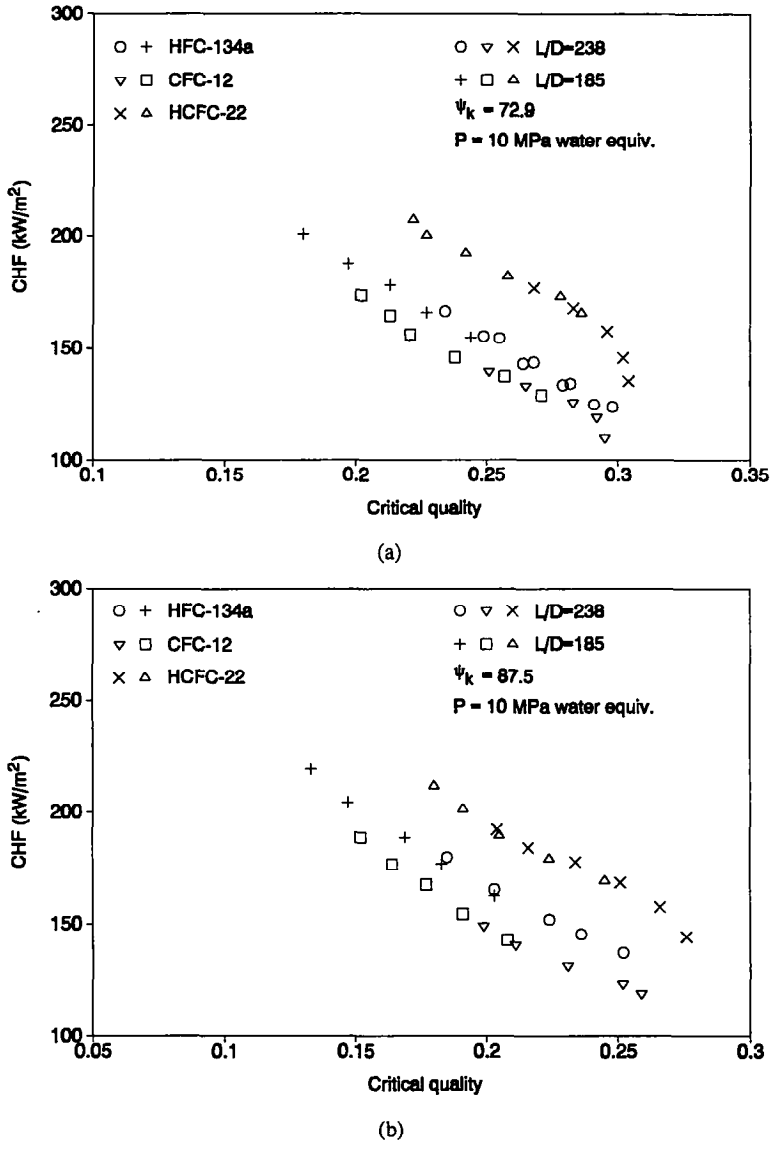


FIG. 4. Effect of quality on CHF for CFC and CFC alternatives at 10 MPa water-equivalent pressure: (a) $\psi_k = 72.9$, (b) $\psi_k = 87.5$.

observed. This may be due to their similar thermophysical properties. However, at high pressure condition as shown in Fig. 4, the difference in CHF values between HFC-134a and CFC-12 becomes larger probably due to a strong effect on properties at high pressure. Also, at high quality and high pressure condition, a tendency towards the 'limiting quality' phenomenon (Doroshchuk *et al.* [18]) was observed. At most pressures and flow conditions, the effect of the ratio of heated length to diameter ($L/D$) is not significant for $L/D$ between 119 and 238.

## DISCUSSION

*Fluid-to-fluid modelling of CHF*

Strictly speaking, in fluid-to-fluid modelling, geometric, thermodynamic and hydrodynamic similarities are necessary. Usually, by using the same $L/D$ ratio in model and prototype, geometric similarity is achieved, i.e.

$$\left(\frac{L}{D}\right)_M = \left(\frac{L}{D}\right)_W \tag{5}$$

where subscript 'M' denotes the modelling fluid and subscript 'W' indicates the equivalent value for water or prototype system. Thermodynamic similarity can be achieved when qualities in both systems are the same at any axial location ($z/D$) along the length, i.e.

$$X(z)_M = X(z)_W. \tag{6}$$

Since from the heat balance equation

$$X(z) = 4\left(\frac{\phi_c}{\lambda G}\right)\left(\frac{z}{D}\right) - \left(\frac{\Delta H_i}{\lambda}\right) \tag{7}$$

the following non-dimensional groups must also be equal:

$$Bo = \left(\frac{\phi_c}{\lambda G}\right)_M = \left(\frac{\phi_c}{\lambda G}\right)_W \quad (8)$$

and

$$\left(\frac{\Delta H_i}{\lambda}\right)_M = \left(\frac{\Delta H_i}{\lambda}\right)_W. \quad (9)$$

For hydrodynamic similarity, a similar density ratio in both systems is needed, i.e.

$$\left(\frac{\rho_f}{\rho_g}\right)_M = \left(\frac{\rho_f}{\rho_g}\right)_W \quad (10)$$

as well as the non-dimensional mass flux in both systems

$$G^*_M = G^*_W \quad (11)$$

where $G^*$ is derived based on the fundamental dimensional analysis associated with experimental evidences and can be expressed in various ways, depending on the investigators such as Stevens and Kirby [19], Dix [20] and Ahmad [9]. Since Ahmad's scaling parameter is considered as the most well developed modelling technique, the CHF data from present work therefore are used to examine the validity of such modelling technique.

*Examination of scaling law*

Based on the fundamental dimensional analysis associated with the selected experimental data, Ahmad [9] developed a scaling parameter ($\psi_{CHF} = G^*$) to model the CHF for different fluids and for various geometries. The $\psi_{CHF}$ is written as

$$\psi_{CHF} = \psi_\sigma = \left(\frac{GD^{1/2}}{\rho_f^{1/2}\sigma^{1/2}}\right)^{1.333} \times \left(\frac{GD}{\mu_f}\right)^{-0.133} \times \left(\frac{GD}{\mu_g}\right)^{-0.2} \quad (12)$$

and, for the fluids whose surface tensions are not known, the alternative form is

$$\psi_{CHF} = \psi_\gamma = \left(\frac{GD}{\mu_f}\right) \times \left(\frac{\gamma^{1/2}\mu_f}{D\rho_f^{1/2}}\right)^{2/3} \times \left(\frac{\mu_f}{\mu_g}\right)^{1/8}. \quad (13)$$

Ahmad postulated that, if the dimensionless parameters, $\rho_f/\rho_g$, $\Delta H_i/\lambda$, $L/D$ and $\psi_{CHF}$ are the same for both fluids, the dimensionless CHF (boiling number, equation (8)) should be equal for both fluids. Then, he showed that the $Bo$ vs $\psi_{CHF}$ for different fluids fall on the same curve for fixed $\rho_f/\rho_g$, $\Delta H_i/\lambda$ and $L/D$. Therefore, the CHF data from present work are used to apply Ahmad's scaling law. Figures 5 and 6 show the scaling curve drawn manually from the data of present work when applying Ahmad's scaling parameter. Most data fall close to the same curve, but some scatter points have been observed perhaps due to the value of $\Delta H_i/\lambda$ being not exactly the same for all data. In addition, the Fig. 1 in Ahmad's [9] paper has been compared with current data and very good agreement can be seen in Fig. 7.

*Comparison with prediction methods*

The CHF results from present work are compared with Groeneveld *et al.*'s [8, 11] and Shah's [13] prediction methods. This is because both prediction methods have been tested for very wide ranges of pressure, tube diameter, heated length, mass velocity and critical quality. Also both methods require the

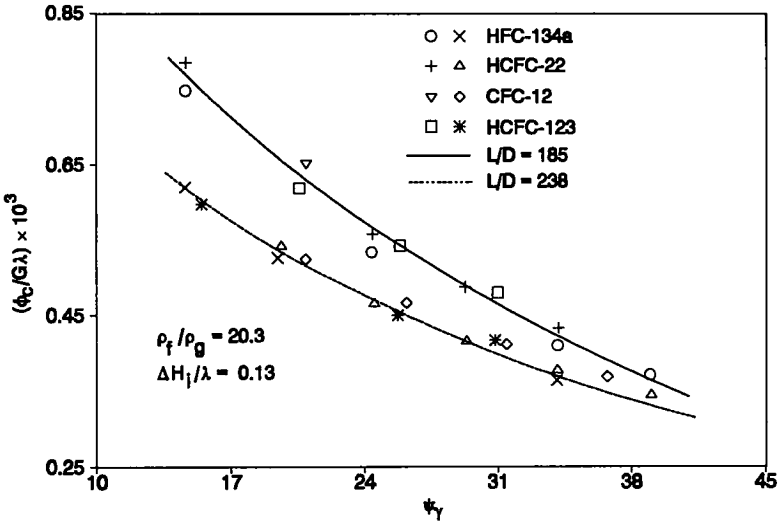


FIG. 5. Comparison of HFC-134a, HCFC-22, CFC-12 and HCFC-123 data at 7 MPa water-equivalent pressure.

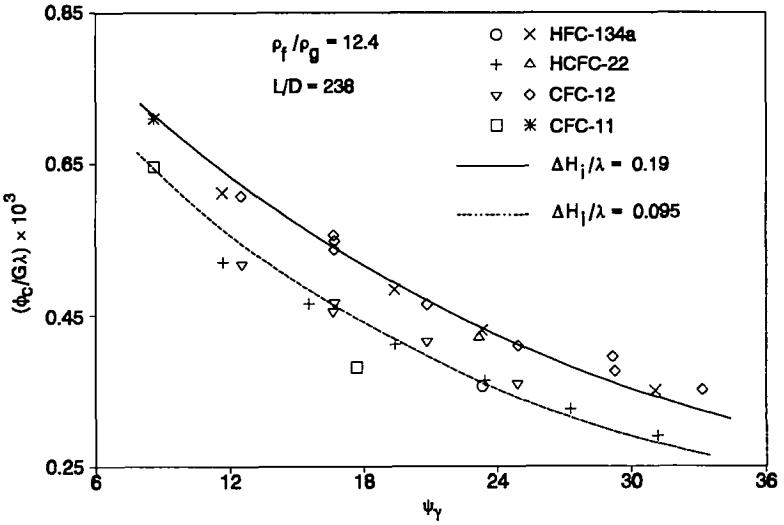


FIG. 6. Comparison of HFC-134a, HCFC-22, CFC-12 and CFC-11 data at 10 MPa water-equivalent pressure.

fluid-to-fluid modelling technique to predict the CHF for non-aqueous fluids.

1. *Groeneveld et al.'s table method.* The CHF table presented by Groeneveld *et al.* [8] is based on the local conditions. It presents the CHF for water in tabular form for discrete values of pressure ($P$), mass flux ($G$) and critical quality ($X_c$). The table was derived for an 8 mm tube with vertical upflow of water by statistically averaging the experimental CHF values within each $P$, $G$ and $X_c$ interval. Groeneveld *et al.* also suggested that CHF values for a tube of $D \neq 8$ mm can be obtained empirically from

$$\mathrm{CHF}_{D\neq 8\,\mathrm{mm}} = \mathrm{CHF}_{8\,\mathrm{mm}}\left(\frac{8}{D}\right)^{1/3} \tag{14}$$

for $2 \leqslant D \leqslant 16$ mm. Linear interpolation is required for non-table $P$, $G$ and $X_c$ values. CHF values for fluids other than water also can be produced from this table method. It requires the use of fluid-to-fluid modelling technique (Groeneveld *et al.* [11]).

Employing the thermodynamic and hydrodynamic similarities, equations (6) and (10), the boiling number, equation (8), is assumed to be equal in both fluids if the $G^*$ values are the same in both fluids. For $G^*$, Ahmad's scaling parameters ($\psi_\sigma$ and $\psi_\gamma$) and Katto's (Katto and Ohno [10]) scaling parameter ($\psi_k$) can be applied, where Katto's scaling parameter is written as

$$\psi_k = \sqrt{\left(\frac{G^2 D}{\sigma \rho_f}\right)}. \tag{15}$$

Groeneveld *et al.* [11] concluded that the prediction

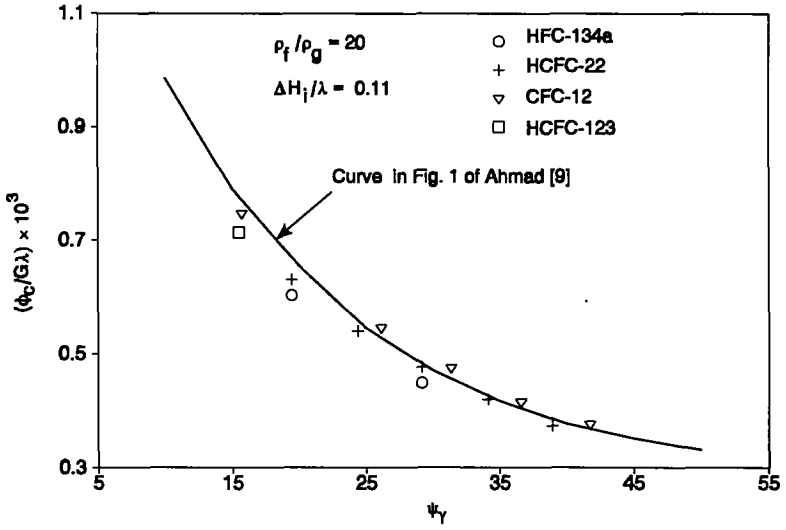


FIG. 7. Comparison of HFC-134a, HCFC-22, CFC-12 and HCFC-123 data with Ahmad's fitted curve at 7 MPa water-equivalent pressure.

errors by using the three scaling parameters are approximately equal. Hence, the use of $\psi_k$ in the present work is recommended because of its simpler form. Once the similarities of all the modelling parameters are achieved, the CHF for non-aqueous fluid can be calculated by using equation (8), i.e.

$$\phi_{c,M} = \left(\frac{\phi_c}{G\lambda}\right)_w \cdot (G\lambda)_M. \quad (16)$$

2. *Shah's empirical correlation.* In 1979 Shah developed a graphical approach for predicting the CHF for a variety of fluids. Shah [13] subsequently modified his approach and developed a correlation of the form

$$\frac{\phi_c}{G\lambda} = f\left(Y, \frac{L}{D}, P_r, \frac{\Delta H_i}{\lambda}, x_c\right) \quad (17)$$

where $P_r$ is the reduced pressure and $Y$ is Shah's correlating parameter, which is written as

$$Y = Pe\, Fr^{0.4}\left(\frac{\mu_f}{\mu_g}\right)^{0.6} \quad (18)$$

where

$$Pe = \frac{G \cdot D \cdot Cp_f}{K_f} \quad \text{(Peclet number)} \quad (19)$$

$$Fr = \frac{G^2}{\rho_f^2 \cdot g \cdot D} \quad \text{(Froude number).} \quad (20)$$

Shah's [13] correlation has been compared to CHF data for 23 types of fluids from 62 independent data sources resulting in an overall mean deviation of 16%.

In Shah's correlation, the CHF is divided into the upstream condition correlation (UCC) and the local condition correlation (LCC). In UCC, the CHF depends primarily on the effect of inlet subcooling. However, in the LCC the CHF depends on the local quality. The detailed procedure to determine the CHF in UCC or LCC can be seen in Shah [13]. Shah [12] compared his correlating parameter ($Y$) with Ahmad's scaling parameter ($\psi_\gamma$) as shown below

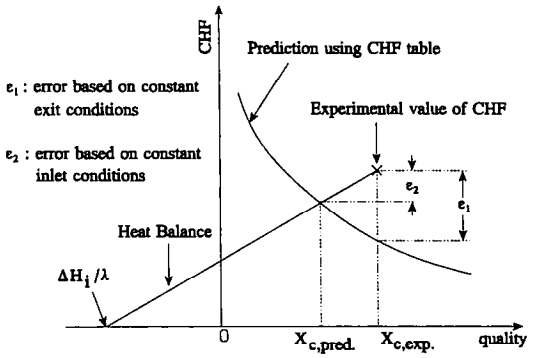


FIG. 8. Errors based on constant exit and constant inlet conditions.

$$Y = G^{1.8} D^{0.6}\left(\frac{Cp_f}{K_f \rho_f^{0.8} g^{0.4}}\right)\left(\frac{\mu_f}{\mu_g}\right)^{0.6} \quad (21)$$

and

$$\psi_\gamma^{1.8} = G^{1.8} D^{0.6}\left(\frac{\gamma^{0.6}}{\rho_f^{0.6} \mu_g^{0.225} \mu_f^{0.375}}\right). \quad (22)$$

Shah [12] concluded that both parameters are identical in $G$ and $D$, but are different in property functions. Shah also concluded that the use of $P_r$ appears to be no different from using the $\rho_f/\rho_g$ to determine the CHF for $P_r \leqslant 0.9$. Shah chose $P_r$ because it is easier to calculate.

3. *Results of comparison.* The comparisons are summarized in Table 6 where the CHF predicted by Groeneveld *et al.* is based on constant inlet condition. CHF prediction errors based on local critical quality ($X_c$) are erroneous because $X_c$ is an experimentally obtained value and is therefore not known prior to the experiment. As illustrated in Fig. 8, the prediction

Table 6. Comparisons of CHF test result with predictions

| Fluid | Pressure (MPa of water equiv.) | No. of data | Groeneveld *et al.* Avg. error (%) | Groeneveld *et al.* R.M.S. error (%)‡ | Shah Avg. error (%)‡ | Shah R.M.S. error (%)‡ |
|---|---|---|---|---|---|---|
| HCF-134a | 7 | 65 | 0.57 | 4.09 | −7.74 | 9.08 |
| | 10 | 73 | −7.94 | 8.31 | −3.37 | 7.23 |
| HCFC-22 | 7 | 68 | −3.53 | 5.36 | −9.27 | 10.24 |
| | 10 | 61 | −7.41 | 8.37 | 3.52 | 6.70 |
| CFC-12 | 7 | 58 | −2.94 | 4.77 | −10.08 | 11.01 |
| | 10 | 69 | −8.75 | 9.26 | −2.30 | 7.50 |
| HCFC-123 | 7 | 60 | −1.68 | 2.68 | −3.39 | 6.53 |
| | 10 | — | — | — | — | — |
| CFC-11 | 7 | 1 | 0.29 | 0.29 | 15.35 | −15.35 |
| | 10 | 6 | 0.92 | 7.55 | 10.31 | 19.21 |

† Avg. error $= \sum_1^N \frac{CHF_{predicted} - CHF_{measured}}{CHF_{measured}} \times 100\%$.

‡ R.M.S. error $= \sqrt{\left(\sum_1^N \left(\frac{CHF_{predicted} - CHF_{measured}}{CHF_{measured}}\right)^2\right)} \times 100\%$.

error should be evaluated based on constant inlet conditions and by satisfying the heat balance equation, equation (7). In general, both Groeneveld *et al.*'s and Shah's methods gave satisfactory predictions when compared to the present test results. For low pressure conditions, Groeneveld *et al.*'s table method shows a better prediction than Shah's correlation. However, at high pressure conditions, Shah's correlations give slightly better results. The large error for CFC-11 may be attributed to a limited data base. Note that the CHF calculation from Shah's correlation requires many transport properties of the fluid (liquid viscosity, vapour viscosity and liquid thermal conductivity) whose evaluation may be subject to uncertainty. Thus, this could affect prediction accuracy of Shah's method. The calculations of $\psi_\gamma$ and $\psi_\sigma$ encounter a similar problem. The liquid viscosity for HFC-134a and HCFC-123 used in the present work are calculated or extrapolated from the correlations of Shankland *et al.* [21] and Kumagai and Takahashi [22], respectively. The rest of the transport properties required for the two fluids are approximated from Wong *et al.*'s [23] general property code. The transport properties of HCFC-22 and CFC-12 are based on the same property source as that used by Shah.

## CONCLUSION

A number of CHF data for CFCs and CFC alternatives were obtained from the present work. The CHF tests were performed in a 4.2 mm I.D. test section with heated length varying from 0.5 to 1 m. The mass flux range covers from 1000 to 4000 kg $m^{-2} s^{-1}$ and the pressure from 1 to 2 MPa simulating water pressure from 7 to 10 MPa. The critical quality range is from 0.07 to 0.6. Due to the high-quality flow conditions, most present CHF data belong to the dryout type from the annular flow regime. Applying Ahmad's scaling law, CHF data for CFCs and CFC alternatives fall closely on the same curve for boiling number vs $\psi_{CHF}$, implying that CFC alternatives can replace CFCs for CHF modelling application. The existing CHF prediction methods yield good agreement with present experimental data as shown in Table 6. In Groeneveld *et al.*'s predicting method, the CHFs for water equivalent and for non-aqueous fluids are calculated in the process through the fluid-to-fluid modelling technique associated with Katto's scaling parameter ($\psi_k$). Thus one of the objectives of the present investigations is also achieved, i.e. to predict the water-equivalent CHF value from a non-aqueous fluid CHF. Finally, it is concluded that HFC-134a, HCFC-123 and HCFC-22 are suitable replacement fluids for CFCs in CHF fluid-to-fluid modelling studies. Similar CHF experimental results for a tubular test section of 8 mm I.D. with varying length using HCFC-22 and CFC-12 were obtained at Chalk River Laboratories, Canada and Kernforschungszentrum Karlsruhe, Germany [24].

*Acknowledgements*—The authors would like to thank the Atomic Energy of Canada Limited and the National Science and Engineering Research Council for their financial support. The donation of HCFC-123 from Du Pont Canada is also much appreciated.

## REFERENCES

1. P. B. Whalley, P. Hutchinson and G. F. Hewitt, The calculation of critical heat flux in forced convection boiling, *Proceedings of the 5th International Heat Transfer Conference*, Vol. 4, pp. 290–294, Tokyo (Sept. 1974).
2. P. B. Whalley, P. Hutchinson and P. W. James, The calculation of critical heat flux in complex situations using an annular flow model, *Proceedings of the 6th International Heat Transfer Conference*, Vol. 5, pp. 65–70, Toronto (Aug. 1978).
3. J. Weisman and B. S. Pei, Prediction of critical heat flux in flow boiling at low qualities, *Int. J. Heat Mass Transfer* **26,** 1463–1477 (1983).
4. C. H. Lee and I. Mudawwar, A mechanistic critical heat flux model for subcooled flow boiling based on local bulk flow conditions, *Int. J. Multiphase Flow* **14,** 711–728 (1988).
5. Y. Katto, A physical approach to critical heat flux of subcooled flow boiling in round tubes, *Int. J. Heat Mass Transfer* **33,** 611–620 (1990).
6. Y. Katto, Prediction of critical heat flux of subcooled flow boiling in round tubes, *Int. J. Heat Mass Transfer* **33,** 1921–1928 (1990).
7. Y. Katto, A prediction model of subcooled water flow boiling CHF for pressure in the range 0.1–20 MPa, *Int. J. Heat Mass Transfer* **35,** 1115–1123 (1992).
8. D. C. Groeneveld, S. C. Cheng and T. Doan, 1986 AECL-UO critical heat flux lookup table, *Heat Transfer Engng* **7**(1–2), 46–62 (1986).
9. S. Y. Ahmad, Fluid to fluid modelling of critical heat flux: A compensated distortion model, *Int. J. Heat Mass Transfer* **16,** 641–662 (1973).
10. Y. Katto and H. Ohno, An improved version of the generalized correlation of critical heat flux for the forced convective boiling in uniformly heated vertical tubes, *Int. J. Heat Mass Transfer* **27,** 1641–1648 (1984).
11. D. C. Groeneveld, B. P. Kiameh and S. C. Cheng, Prediction of critical heat flux (CHF) for non-aqueous fluids in forced convective boiling, *Proceedings of the 8th International Heat Transfer Conference*, Vol. 5, pp. 2209–2214, San Francisco (1986).
12. M. M. Shah, A generalized graphical method for predicting CHF in uniformly heated vertical tubes, *Int. J. Heat Mass Transfer* **22,** 557–568 (1979).
13. M. M. Shah, Improved general correlation for critical heat flux during upflow in uniformly heated vertical tubes, *Int. J. Heat Fluid Flow* **8,** 326–335 (1987).
14. K. Watanabe, Current status of thermophysical properties research on CFC alternatives, *Proceedings of 3rd International Energy Agency Heat Pump Conference*, pp. 263–282, Tokyo, Japan (1990).
15. N. Hammouda, Private communication (1992).
16. N. Hammouda, S. C. Cheng and D. C. Groeneveld, Evaluation of thermophysical properties of Freon-22, in press by *Wärme- und Stoffübertragung*.
17. M. O. McLinden, J. S. Gallagher, L. A. Weber, G. Morrison, D. Ward, A. R. H. Goodwin, M. R. Moldover, J. W. Schmidt, H. B. Chae, T. J. Bruno, J. F. Ely and M. L. Huber, Measurement and formulation of the thermodynamic properties of refrigerants 134a (1,1,1,2-tetrafluoroethane) and 123 (1,1-dichloro-2,2,2-trifluoroethane), *ASHRAE Trans.* **95,** Pt. 2, 263 (1989).
18. V. E. Doroshchuk, F. P. Lantsman and L. L. Levitan, A peculiar type of burnout in evaporative tubes, *Pro-*

*ceedings of the 4th International Heat Transfer Conference*, Vol. 6, Paper B6.1, Paris (1970).
19. G. F. Stevens and G. J. Kirby, A quantitative comparison between burn-out data for water at 1000 lb/in$^2$ and Freon-12 at 155 lb/in$^2$ (ABS) uniformly heated round tubes, vertical upflow, *AEEW-R327* (1964).
20. G. E. Dix, Freon–water modelling of critical heat flux in round tubes, ASME paper No. 70-HT-26 (1970).
21. I. R. Shankland, R. S. Basu and D. P. Wilson, Thermal conductivity and viscosity of a new stratospherically safe refrigerant—1,1,1,2-tetrafluoroethane (R-134a), *Proceedings of the Meeting of Commission B1, B2, E1, E2 of the IIR*, Purdue University (1988).
22. A. Kumagai and S. Takahashi, Viscosity of saturated liquid fluorocarbon refrigerants from 273 to 353 K, *Int. J. Thermophys.* **12,** 105–117 (1991).
23. Y. L. Wong, S. C. Cheng and D. C. Groeneveld, Generalized thermodynamic and transport properties evaluation for nonpolar fluids, *Heat Transfer Engng* **11,** 60–71 (1990).
24. D. C. Groeneveld, D. Blumenroehr, S. C. Cheng, X. Cheng, S. Doerffer, F. J. Erbacher, R. M. Tain and W. Zeggel, CHF fluid-to-fluid modelling studies in three laboratories using different modelling fluids, *Proceedings of NURETH-5*, Vol. 2, pp. 531–538, Salt Lake City, Utah (Sept. 1992).